Journal of the Korean Electrochemical Society
Vol. 9, No. 2, 2006, 77-83

Effect of Anodic Gas Compositions on the Overpotential in a Molten Carbonate Fuel Cell

C.-G. Lee*, D.-H. Kim†, S.-U. Hong, S.-H. Park, and H.-C. Lim†

Dept. of Chemical Engineering, Hanbat National University, San 16-1, Dukmyung-dong, Yuseong-gu, Daejeon, Korea
†Korea Electric Power Research Institute, 103-16, Munji-dong, Yuseong-gu, Daejeon, Korea

(Received April 28, 2006 : Accepted May 11, 2006)

Abstract : Anodic overpotential has been investigated with gas composition changes in a 100 cm^2 class molten carbonate fuel cell. The overpotential was measured with steady state polarization, reactant gas addition (RA), inert gas step addition (ISA), and electrochemical impedance spectroscopy (EIS) methods at different anodic inlet gas compositions, i.e., H_2:CO_2:H_2O = 0.69:0.17:0.14 atm and H_2:CO_2:H_2O = 0.33:0.33:0.33 atm, at a fixed H_2 flow rate. The results demonstrate that the anodic overpotential decreases with increasing CO_2 and H_2O flow rates, indicating the anode reaction is a gas-phase mass-transfer control process of the reactant species, H_2, CO_2, and H_2O. It was also found that the mass-transfer resistance due to the H_2 species slightly increases at higher CO_2 and H_2O flow rates. EIS showed reduction of the lower frequency semi-circle with increasing H_2O and CO_2 flow rate without affecting the high frequency semi-circle.

Keywords : MCFC, Anode, Gas composition, Overpotential.

1. Introduction

Molten carbonate fuel cells (MCFCs) are based on carbonate electrolyte, which requires a supply of CO_2 to the anode and cathode electrodes to prevent the carbonate electrolyte from decomposition, because the carbonate melts are in equilibrium with oxide ions and CO_2. In addition, the CO_2 presence with H_2 at the anode produces CO according to the water-gas-shift reaction ($H_2+CO_2=H_2O+CO$), and finally carbon at the deficient of H_2O species. The carbon deposition in the MCFC obstructs gas flow and electrode reactions, which shortens the life of fuel cell. Water addition is a general means to prevent this problem. Thus, the anode gases are composed of H_2, CO_2, and H_2O at the MCFC anode.

The high temperature melting carbonate electrolyte allows the use of CO as a fuel in the MCFC. However, the oxidation rate of CO in the carbonate melts is too slow to be used.[1] A practical way of utilizing CO is to supply it with steam, because the water-gas-shift reaction is a fast reaction in the gas phase and the water addition results in H_2 production.[2] Similar output voltages have been reported in H_2 fuel and fuel employed a mixed gas of CO and H_2O.[3] The use of CO as a fuel in the MCFC opens up the possibility of utilizing a coal based electric power source, as CO is one of the major component in coal gas. On the other hand, to date, steam reforming of natural gas is the most competitive technology because of the well established infrastructure of the natural gas supply and maturity of the steam reforming technology with economic compatibility. The steam reforming of natural gas at 750°C yields approximately 75.1% of H_2, 12.5% of CO, 10.3% of CO_2, and 2.1% of CH_4 at a steam to carbon ratio of 3 based on the dry condition, which is the general gas composition at the anode of the MCFC.

Ang and Sammells have reported that the anode is a multicomponent reaction system of H_2, CO_2, and H_2O species (Eq. 1).[4]

$$i_o \propto P(H_2)^{0.25} P(CO_2)^{0.25} P(H_2O)^{0.25} \quad (1)$$

where i_o is the exchange current density, which represents the reaction rate on the electrode surface. The above equation also suggests that the reactant species take part in the anode reaction equally. Based on Eq. (1), Yuh and Selman[5] suggested the following empirical relation of anodic overpotential (Eq. 2) with respect to the partial pressures of these gases with significant uncertainties.

$$\eta_{an} \propto P(H_2)^{-0.42} P(CO_2)^{-0.17} P(H_2O)^{-1.0} \quad (2)$$

On the other hand, Morita *et al*., reported that anodic overpotential is mainly a function of hydrogen partial pressure (Eq. 3).[6]

$$\eta_{an} \propto P(H_2)^{-0.5} \quad (3)$$

It should be noted, however, that these works excluded the flow rate effect on the overpotential. A previous work has suggested that the amount of the CO_2 species provides anodic

*E-mail: leecg@hanbat.ac.kr

overpotential by the gas-phase mass-transfer effect.[7] Recently, Lee *et al*., utilizing an inert gas step addition (ISA) method developed in their laboratory, reported that the anode reaction is a gas-phase mass-transfer control system.[8-10] However, the ISA could not give information on the mass-transfer effect of each reactant species. Another method of reactant gas addition (RA) revealed that the anodic overpotential depends on the flow rates of the H_2, CO_2, and H_2O species.[11]

There have been numerous reports on the characterization of MCFCs with the Electrochemical Impedance Spectroscopy (EIS) method. Some works suggested that two semicircles are obtained at the high and low frequency regions, respectively, in a Cole-Cole plot.[12,13] From the gas composition and utilization changes, it has been suggested that the semi-circle in the high frequency region represents cathodic reaction resistance while the semi-circle in the low frequency region represents anodic polarization.

The present work illuminates the effects of gas-composition change on the anodic overpotential, employing ISA, RA, and EIS methods for 100 cm^2 class MCFC single cells.

2. Experimental

Several 100 cm^2 class MCFC single cells were used in this work. The anode was made of Ni alloy, and the cathode was in-situ oxidized NiO. The cell matrix was $LiAlO_2$ with alumina fiber for reinforcement. The electrolyte was a mixture of 62 mol% Li_2CO_3 and 38 mol% K_2CO_3. The cells were operated at 923 K under atmospheric conditions. More details of the cell preparation and operation have been described in a previous work.[8]

Two gas mixtures, $H_2:CO_2:H_2O$=0.69:0.17:0.14 atm and $H_2:CO_2:H_2O$= 0.33:0.33:0.33 atm, were used for the anode. The gas compositions were prepared by controlling CO_2 and H_2O flow rate at a fixed H_2 flow rate of 0.17 *l*/min. The water flow rate in the anode gas was controlled by adjusting the water temperature of a bubbler. The cathode gas was a mixture of 70 mol% air and 30 mol% CO_2.

Overpotential variation was measured with several methods at different anode gas compositions. First, steady state polarization (SSP) was utilized to record the voltage decline by the current load from the open circuit voltage (OCV); thus the change of the slope by the gas composition change indicated the overpotential variation at the electrode. The current applied to the SSP ranged from 0 to 15 A.

Second, the reactant gas addition (RA) method was employed. As reported in a previous paper,[11] RA adds a reactant gas to the anode, which leads to the partial pressure and flow rate changes of the species. These changes are represented at the OCV and voltage at the current density. Since the difference between the OCV and voltage at a polarization state is the total overpotential, the overpotential change by the gas composition variation indicates the effect of the gas composition on the electrode reaction kinetics. When a reactant gas is added to the anode, the OCV is varied according to the following Nernst equation (Eq. 4) and the voltage at the polarization state is also changed.

$$E_{\mathrm{OCV}} = E_{\mathrm{o}} + \frac{RT}{2F}\ln\left(\frac{[\mathrm{H_2}]}{[\mathrm{H_2O}][\mathrm{CO_2}]_{an}}[\mathrm{O_2}]^{0.5}[\mathrm{CO_2}]_{ca}\right) \quad (4)$$

When we assume the OCV variation is ΔE and the voltage variation is ΔV_{P}, the difference ($\Delta V = \Delta V_{\mathrm{P}} - \Delta E$) between ΔE and ΔV_{P} represents the overpotential variation by the reactant addition.[11] A positive ΔV indicates that the overpotential is reduced by the addition and the reactant addition enhances the electrode reaction rate. On the contrary, a negative ΔV indicates that the overpotential rises by the addition and the addition reduces the mass-transfer rate. More details of the RA measurement have been described in a previous work.[11]

The third measurement technique was the inert gas step addition (ISA) method. ISA adds inert gas to an electrode, which results in flow rate changes of the reactant gases.[8] The flow rate change results in the overpotential variation, and thus the overpotential as a function of flow rate yields information of the flow-rate-induced overpotential at the electrode. Since the inert gas addition port is placed several meters from the cell in the ISA measurements, a certain amount of inert gas addition increases the reactant gas flow rate until the added inert gas arrives at the cell. During this time region the inert gas does not flow in the cell, and thus the voltage shift at the time range is solely attributed to the reactant flow rate. Since the reactant flow rate corresponds to the utilization at a fixed current load, the voltage shift can be expressed by the utilization, which is a ratio of the required reactant amount according to Faraday's law to the fed reactant amount. In a previous work,[8] the following relations were suggested (Eq. 5). The anodic overpotential is comprised of overpotentials due to each reactant species,

$$\eta_{\mathrm{an}} \cong q_{\mathrm{H_2}} u_{\mathrm{H_2}}^{0.5} + q_{\mathrm{CO_2}} u_{\mathrm{CO_2}}^{0.5} + q_{\mathrm{H_2O}} u_{\mathrm{H_2O}}^{0.5} \quad (5)$$

where $q_{\mathrm{A}}=1.51[RT(iLs)^{1/2}\nu_{\mathrm{A}}^{1/6}/(n^3F^3a^2c_{0,\mathrm{A}})^{1/2}D_{G,A}^{2/3}]$, and the subscript A denotes H_2, CO_2, and H_2O, i is the current, L is the electrode length, s is the cross-sectional area of the gas channels, ν is the kinematic viscosity, a is the geometrical surface area, D_{G} is the gas-phase diffusivity, and other symbols have their usual meaning.

Then, $\eta_{\mathrm{an}} \cong q_1 u_{\mathrm{H_{2,1}}}^{0.5}$ (6)

where $q_{\mathrm{H_2}} = q_1 + \xi_1^{0.5} q_{\mathrm{CO_2}} + \xi_2^{0.5} q_{\mathrm{H_2O}}$, $u_{\mathrm{CO_2}} = \xi_1 u_{\mathrm{H_2}}$, $u_{\mathrm{H_2O}} = \xi_2 u_{\mathrm{H_2}}$

Finally, the voltage shift by the utilization change can be expressed as follows,

$$\Delta V_{\mathrm{I}} = V_2 - V_1 = \eta_{\mathrm{an},1} - \eta_{\mathrm{an},2} = q_1 u_{\mathrm{H_{2,1}}}^{0.5} - q_1 u_{\mathrm{H_{2,2}}}^{0.5} \quad (7)$$

If $m_1 = q_1 u_{\mathrm{H_{2,1}}}^{0.5}$, then

$$\Delta V_{\mathrm{I}} = m_1 - q_1 u_{\mathrm{H_{2,2}}}^{0.5} \quad (8)$$

More details can be found in a previous work.[8]

Electrochemical Impedance Spectroscopy (EIS) was con-

ducted with a Solartron 1287 Interface and a Solartron 1260 frequency response analyzer. Frequency was scanned from 1000 Hz to 0.1 Hz with 5 mV rms at an open circuit state.

3. Results and Discussion

According to Eq. (5), the anodic overpotential is the sum of the flow-rate-induced overpotentials of each reactant species. Thus, a large flow rate of the species reduces utilization and anodic overpotential. This assumption is demonstrated with different flow rates of the species. Fig. 1 shows some results of steady state polarization at a standard anode gas inlet composition, $H_2:CO_2:H_2O = 0.69:0.17:0.14$ atm and an equal composition $H_2:CO_2:H_2O = 0.33:0.33:0.33$ atm. Lower OCV is observed at the equal composition than at the standard gas composition due to the increased CO_2 and H_2O partial pressures. Table 1 compares the measured and calculated OCVs according to Eq. (4). Good agreement is observed between the measured and calculated OCVs.

With increasing current density, a voltage decrease is observed. The difference between OCV and voltage at the polarization state is the total voltage loss (η). The total voltage loss is ascribed to the ohmic loss due to the electrical resistance at the cell components and overpotential due to the electrochemical reaction resistance at the electrodes. A milder voltage slope is observed at the equal gas composition, which indicates the total voltage loss at the equal gas composition is less than that at the standard gas composition ($\eta_{Eql} < \eta_{Std}$). This implies that the anode gas composition affects the anodic overpotential, and the overpotential decreases at higher H_2O and CO_2 flow rates.

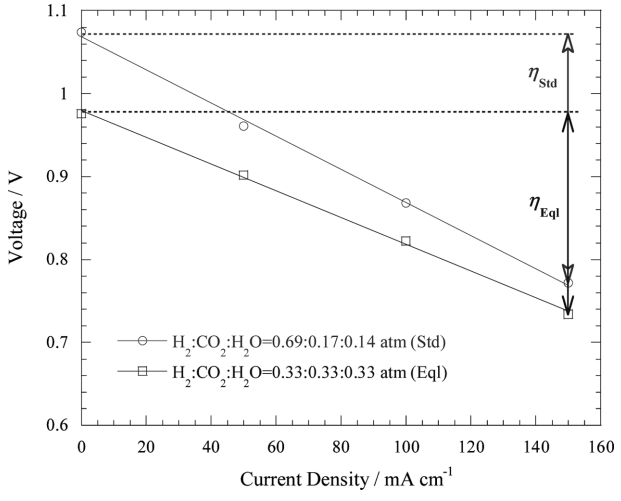

Fig. 1. Steady state polarization results with different anode gas compositions of $H_2:CO_2:H_2O = 0.69:0.17:0.14$ atm (called Standard gas composition) and $H_2:CO_2:H_2O = 0.33:0.33:0.33$ atm (called Equal gas composition) at a 0.17 *l*/min of fixed H_2 flow rate, cathode flow rate of 0.883 *l*/min (Air:CO_2 = 0.7:0.3 atm), 923 K, 1 atm.

Table 1. Comparisons of calculated and measured OCV at the standard gas composition ($H_2:CO_2:H_2O = 0.69:0.17:0.14$ atm) and equal gas composition ($H_2:CO_2:H_2O = 0.33:0.33:0.33$ atm) at the cathode gas composition of Air:CO_2 = 0.7:0.3 atm, 923 K, 1 atm.

	Calculated OCV / V	Measured OCV / V
Standard gas	1.073	1.074
Equal gas	0.969	0.976

It has been suggested that the anode reaction is mainly a gas-phase mass-transfer control process and each reactant species can be attributed to the anodic overpotential.[8)]

$$\eta_{an} = \eta_{H_2} + \eta_{CO_2} + \eta_{H_2O} \cong \sum_A i \frac{RT}{n^2 F^2 a c_{0,A}} \left(\frac{1}{k_{G,A}}\right) \quad (9)$$

where subscript A denotes H_2, CO_2, and H_2O reaction species, and $k_{G,A}$ ($\equiv 0.664(\upsilon_{f,A}/L)^{1/2}(D_{G,A})^{2/3}(\nu_A)^{1/6}$) is a gas-phase mass-transfer coefficient. In this equation, a is the geometrical surface area, $\upsilon_{f,A}$ is the gas velocity, L is the electrode length, $D_{G,A}$ is the gas-phase diffusivity, ν is the kinematic viscosity, and other subscripts have their usual meaning.

In addition, RA measurement revealed that considerable overpotential due to the CO_2 and H_2O species existed at a standard anode gas composition ($H_2:CO_2:H_2O = 0.69:0.17:0.14$ atm) compared with H_2 species.[11)] Further, overpotential depended on the flow rate rather than the partial pressure of the species.

A previous work reported that RA measurement yields information on the overpotential induced by each reactant species.[11)] Fig. 2 provides a comparison of the RA results by the addition of 0.3 *l*/min of CO_2 to the standard and equal anode gas compositions. At an open circuit state, the CO_2 addition decreases OCV according to Eq. (4). Since the addition port is located at a distance from the cell, the OCV reduction occurs after several seconds delay. The OCV difference before and after the addition is represented by ΔE. At a polarization state, two voltage peaks, at 5 and 40 seconds, which were ascribed to the flow rate change of the reactants by the addition, are observed. A voltage decrease by the CO_2 addition is also obtained at around 20 seconds. The voltage difference at a polarization state before and after the addition is ΔV_P. Thus, ΔV ($=\Delta V_P - \Delta E$) represents kinetic information by the addition of a reactant species in terms of the overpotential. A positive ΔV value indicates that the overpotential decreases by the reactant gas addition due to the enhanced mass-transfer rate. From Fig. 2(a), ΔE is more negative than ΔV_P, which leads to a positive ΔV. Thus, the CO_2 addition to the anode reduces the mass-transfer resistance of the CO_2 species. The RA measurement at equal gas composition (Fig. 2b) shows similarity between OCV and voltage shift patterns by 0.3 *l*/min of CO_2 addition. Since the total flow rate of the equal composition (ca. 0.51 *l*/min) was about two times the standard composition (ca. 0.25 *l*/min), the partial pressure change at the equal gas composition is relatively small compared with that at the standard composition by 0.3 *l*/min of CO_2 addition. This leads to a small OCV decrease and voltage shifts, as shown in Fig. 2(b). Faster voltage relaxations at around 10 and 50 seconds as well as narrower voltage peaks at 5 and 35 seconds are also observed at the equal gas composition. Because of the

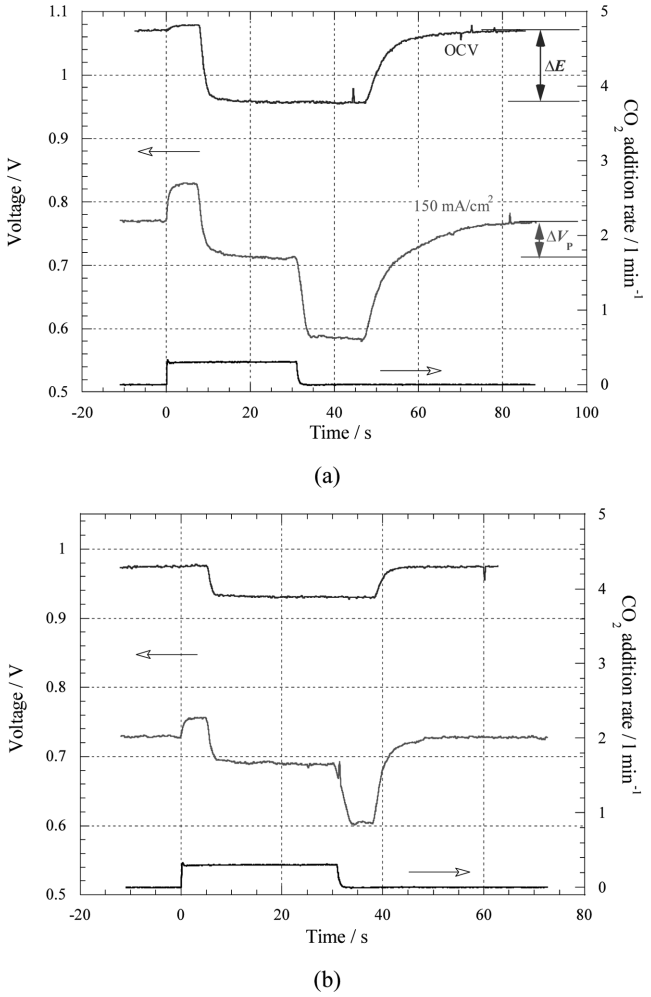

Fig. 2. RA results with 0.3 *l*/min of CO_2 addition to the different anode gas compositions at a 0.17 *l*/min of fixed H_2 flow rate, cathode flow rate of 0.883 *l*/min (Air:CO_2 = 0.7:0.3 atm), 923 K, 1 atm. (a) Standard anode gas composition of H_2:CO_2:H_2O=0.69: 0.17:0.14 atm, (b) Equal gas composition of H_2:CO_2:H_2O=0.33: 0.33:0.33 atm.

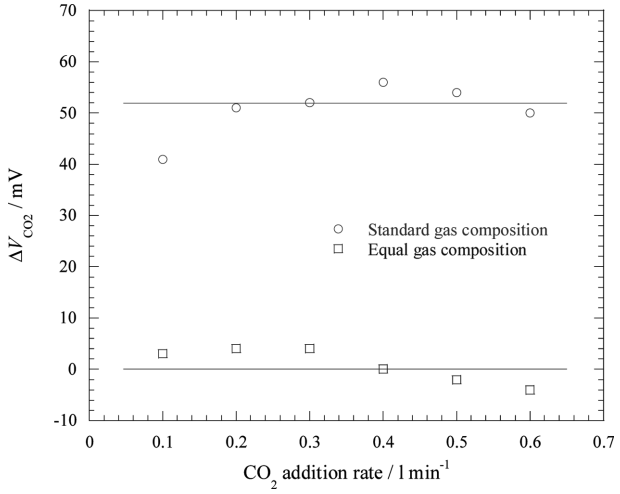

Fig. 3. V_{CO2} with RA measurement as a function of CO_2 addition rate to the standard anode gas composition (H_2:CO_2:H_2O = 0.69: 0.17:0.14 atm) and equal gas composition (H_2:CO_2:H_2O = 0.33:0.33 :0.33 atm) at the cathode flow rate of 0.883 *l*/min (Air:CO_2 = 0.7: 0.3 atm), 923 K, 1 atm.

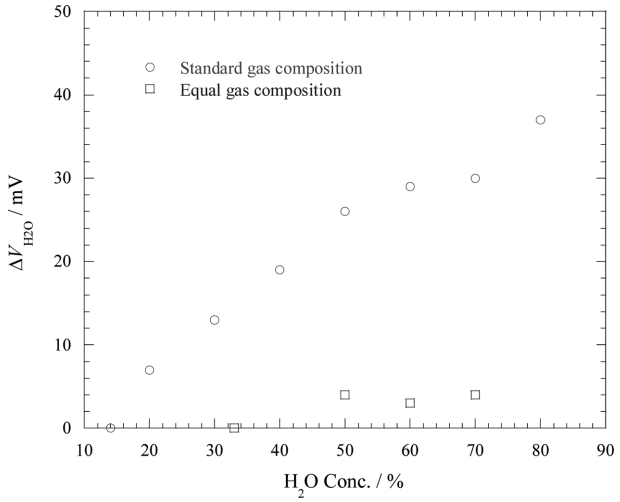

Fig. 4. V_{H2O} with steady state polarization as a function of H_2O concentration at the standard anode gas composition (H_2:CO_2:H_2O = 0.69:0.17:0.14 atm) and equal gas composition (H_2:CO_2:H_2O = 0.33:0.33:0.33 atm) at the cathode flow rate of 0.883 *l*/min (Air: CO_2 = 0.7:0.3 atm), 923 K, 1 atm.

smaller ΔE and ΔV_P, a very small ΔV is expected at the equal gas composition.

Fig. 3 compares ΔV_{CO2} with respect to the CO_2 addition amount at the standard and equal gas compositions. Very high ΔV_{CO2} is observed at the standard composition, whereas ΔV_{CO2} is close to zero at the equal gas composition. The high ΔV_{CO2} at the standard gas composition reflects the existence of considerable overpotential due to the CO_2 species. However, increases in the CO_2 flow rate at the equal gas composition reduce ΔV_{CO2} and overpotential. Independence of ΔV_{CO2} on the CO_2 addition amount also indicates that anodic overpotential has very little dependence on the partial pressure of the reactant species. Negative ΔV_{CO2} values over 0.3 *l*/min of CO_2 addition rate at the equal gas composition are likely due to obstruction of the mass transfer of H_2 and H_2O species by the excess amount of CO_2. These results imply that the large overpotential at the standard composition is attributed to the low flow rate of CO_2 species.

Fig. 4 shows ΔV_{H2O} at the standard and equal gas compositions. Direct quantitative addition of H_2O to the anode is experimentally difficult, thus ΔV_{H2O} was estimated by steady state polarization (SSP). As shown in Fig. 1, the SSP shows OCV and voltage with respect to the current. In principle, $\Delta V_{H2O}=\Delta V_{P,H2O} - \Delta E_{H2O}$; therefore, comparison of the SSP results at the open circuit state and polarization state with a function of different H_2O concentration can give ΔE_{H2O} and $\Delta V_{P,H2O}$, respectively. In this work, the SSP results were obtained at 53°C humidifier temperature, corresponding to 14% of H_2O, and at 90°C humidifier temperature (70% of H_2O). ΔE_{H2O} and $\Delta V_{P,H2O}$ were obtained by comparison with 14% H_2O concentration. At the standard gas composition

ΔV_{H2O} increases with H_2O concentration, indicating significant overpotential exists due to the H_2O species and overpotential decreases with the H_2O concentration. On the contrary, very small ΔV_{H2O} is observed at the equal gas composition. In addition, ΔV_{H2O} shows less dependence on the H_2O concentration, which suggests that a sufficient flow rate of H_2O leads to a very small overpotential due to the species at the anode. These results indicate that the large overpotential due to the H_2O species at the standard composition is attributed to its low flow rate.

Figs. 5 (a) and (b) are RA results by 0.3 *l*/min of H_2 addition to the standard and equal gas compositions. Open circuit voltage increases by the H_2 addition according to Eq. (4). The onset of OCV with several seconds delay is attributed to the installation of the addition port ahead of the cell. At 15 A of polarization state, clear voltage shifts are observed at both gas compositions. In particular, two voltage shoulders are observed, which are due to the flow rate change of the reactants by the H_2 addition. Larger reactant flow rate at the equal gas composition leads to smaller and narrower voltage shoulders. Consequently, the H_2 addition gives clear voltage shifts, ΔE_{H2} and $\Delta V_{P,H2}$, at both gas compositions, and thus ΔV_{H2} can be estimated.

Fig. 6 compares ΔV_{H2} at the standard and equal gas compositions. Contrary to the cases of CO_2 and H_2O addition, larger ΔV_{H2} is observed at the equal gas composition. Since the ΔV_{H2} value represents overpotential due to the species, larger overpotential exists at the equal gas composition. Two explanations are available for this behavior. One is the reduction of the mass-transfer rate of the H_2 species by the increased CO_2 and H_2O at the equal gas composition. According to the Maxwell-Stefan equation, diffusion coefficients at the multi components are affected by the partial pressures of the species.[14] Increased CO_2 and H_2O partial pressures at the equal gas composition lead to a smaller H_2 diffusivity. The other reason is lower H_2 flow rate in the cell at the equal gas composition. The anode gas composition in the cell is balanced by the water-gas-shift reaction ($H_2+CO_2 = H_2O+CO$) as shown in the Table 2, thus the equal compo-

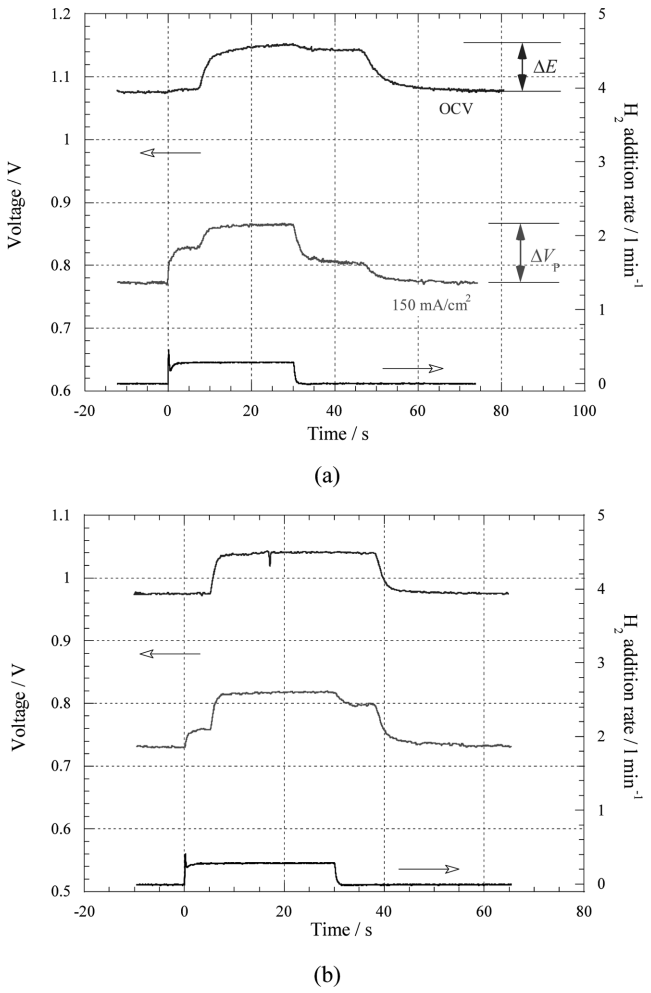

Fig. 5. Results of RA measurement with H_2 addition rate (0.3 *l*/min) to the different anode gas compositions at the cathode flow rate of 0.883 *l*/min (Air:CO_2=0.7:0.3 atm), 923 K, 1 atm. (a) Standard gas composition of H_2:CO_2:H_2O = 0.69:0.17:0.14 atm, (b) Equal gas composition of H_2:CO_2:H_2O = 0.33:0.33:0.33 atm.

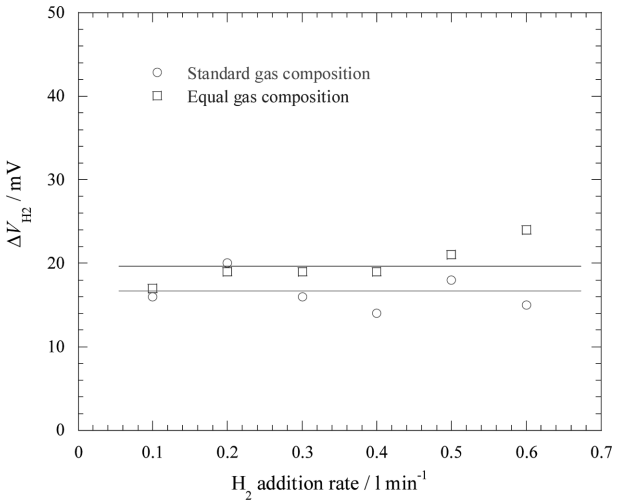

Fig. 6. V_{H2} with RA measurement as a function of H_2 addition rate to the standard gas composition (H_2:CO_2:H_2O=0.69:0.17:0.14 atm) and equal gas composition (H_2:CO_2:H_2O=0.33:0.33:0.33 atm) at the cathode flow rate of 0.883 *l*/min (Air:CO_2=0.7:0.3 atm), 923 K, 1 atm.

Table 2. Anode gas flow rates and compositions in the feed and those in the cell balanced by the water-gas-shift reaction at the standard and equal gas compositions at 923K, 1 atm.

	Feed flow rates and compositions	Balanced flow rates and compositions in the cell
Standard gas	H_2:CO_2:H_2O=0.174:0.043:0.035 *l*/min (=0.69:0.17:0.14 atm)	H_2:CO_2:H_2O:CO=0.149:0.019:0.060:0.025 l/min (=0.59:0.08:0.24:0.10 atm)
Equal gas	H_2:CO_2:H_2O=0.174:0.174:0.174 l/min (=0.33:0.33:0.33 atm)	H_2:CO_2:H_2O:CO=0.132:0.132:0.216:0.042 l/min (=0.25:0.25:0.41:0.08 atm)

sition gives less H_2 flow rate than the standard composition in the cell.

Figs. 7(a) and (b) are inert gas step addition (ISA) results by the addition of 0.4 *l*/min of N_2 to the anode. Two characteristic voltage peaks are observed, which result from flow rate changes by the N_2 addition. Since the inert gas addition port is located at a distance from the cell, the N_2 addition increases the reactant flow rate while nitrogen reaches the cell and results in the "a" peak. The height of the "a" peak (ΔV_I) represents the overpotential decrease by the flow rate increase, as shown in Eq. (7). Since the utilization is the ratio between the required amounts to the fed amount at the current load, the flow rate increase by the N_2 addition reduces the utilization. In addition, the utilization is inversely proportional to the flow rate, and thus the peak height can be expressed as Eq. (8). At the two gas compositions, two voltage peaks are observed. The equal gas composition has a larger flow rate, and thus the same amount of N_2 addition reduces utilization differently and equal gas composition has

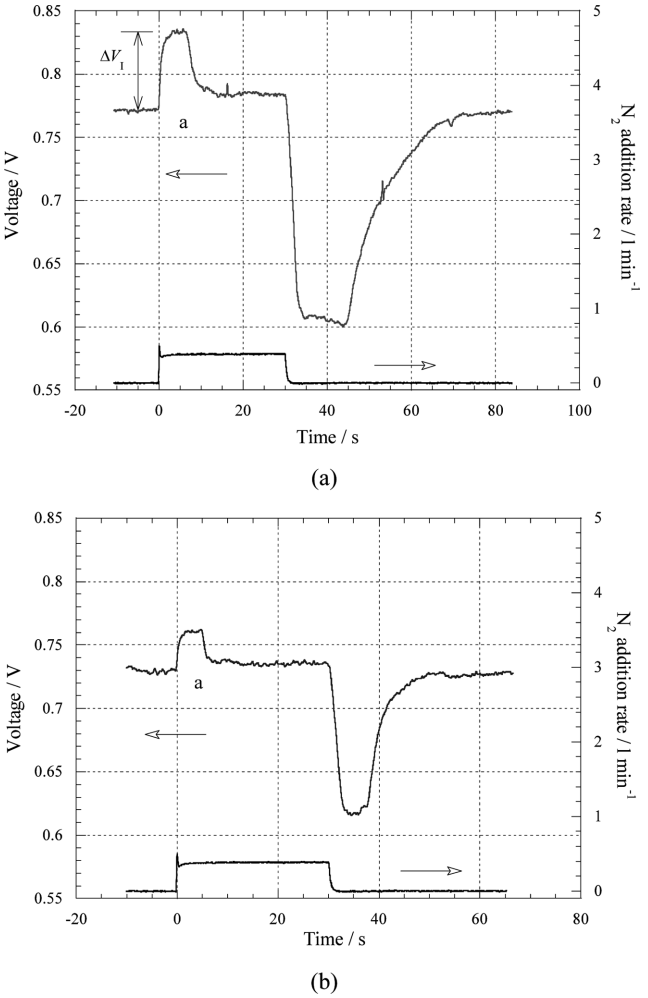

Fig. 7. ISA results at the addition of 0.4 *l*/min N_2 to the different anode gas compositions at the cathode flow rate of 0.883 *l*/min (Air:CO_2=0.7:0.3 atm), 923 K, 1 atm, and 15A of current load. (a) Standard gas composition of H_2:CO_2:H_2O=0.69:0.17:0.14 atm, (b) Equal gas composition of H_2:CO_2:H_2O=0.33:0.33:0.33 atm.

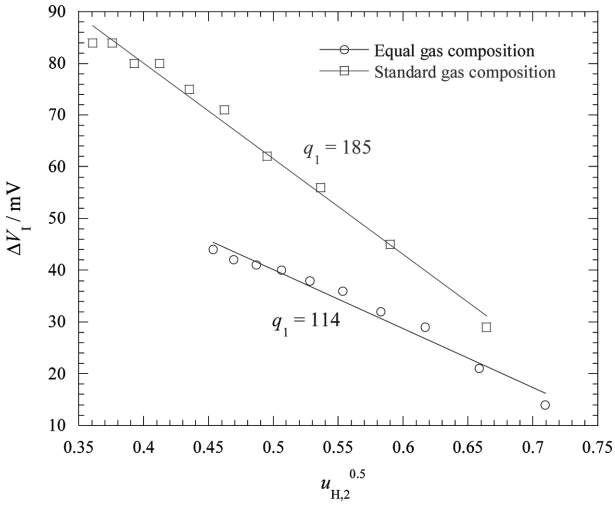

Fig. 8. Relations of Eq. (8) by the addition of N_2 to the standard gas composition (H_2:CO_2:H_2O=0.69:0.17:0.14 atm) and equal gas composition (H_2:CO_2:H_2O=0.33:0.33:0.33 atm).

a smaller utilization shift according to Eq. (10).

$$u_{2,A} = \frac{\upsilon_{c,A}}{\upsilon_{f,A}}\left(\frac{\upsilon_f}{\upsilon_f + \upsilon_i}\right) \tag{10}$$

where $\upsilon_t = \sum_A \upsilon_{t,A}$, subscript A is reactant species, υ_c and υ_f are required and feed flow rate, respectively, and υ_i is the inert gas flow rate. Therefore, a smaller "a" voltage peak is observed at the equal gas composition.

Fig. 8 shows the relation of Eq. (8) with the height of the "a" peak (ΔV_I). At the same N_2 addition range, smaller utilization changes are observed at the equal gas composition. The q_1 value at the standard composition is about 185 mV, which is much larger than the previous result of ca. 159 mV.[10] Since the q_1 value represents the mass-transfer effect through the porous electrode, a larger q_1 value indicates that the anode in this work is likely more complicated and gives lower diffusivity. This suggests that the anode structure may give additional overpotential through the mass-transfer resistance. On the other hand, a much smaller q_1 value of ca. 114 mV is also observed at the equal gas composition, which indicates that the mass-transfer resistance at the anode is mitigated at higher CO_2 and H_2O flow rates. This is in line with the results obtained by SSP and RA measurements in this work.

As another experiment for the anode reaction, Electrochemical Impedance Spectroscopy (EIS) was conducted with a 100 cm^2 class MCFC single cell. In principle, the EIS represents the electrode reaction kinetics and is a powerful tool for kinetic research. Numerous works have been done with EIS measurement in MCFC research. Among them, Lee *et al*., reported two semi-circles ascribed to cathodic and anodic reaction resistances with a 100 cm^2 class MCFC; the high frequency semi-circle reflects the cathodic mass-transfer rate and the low frequency semi-circle represents anodic resistance.[12] Fig. 9 compares the EIS results measured at the two gas compositions, revealing a decrease in the lower fre-

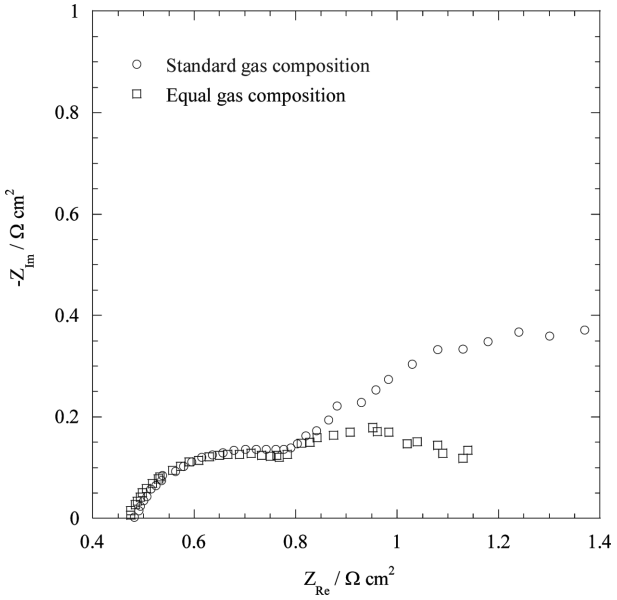

Fig. 9. Cole-Cole plot with EIS measurement at the standard gas composition (H_2:CO_2:H_2O=0.69:0.17:0.14 atm) and equal gas composition (H_2:CO_2:H_2O=0.33:0.33:0.33 atm) in the frequency range of 1 kHz to 0.1 Hz at OCV with 5 mV rms signal and at the cathode flow rate of 0.883 l/min (Air:CO_2=0.7:0.3 atm), 923K, 1 atm.

quency semi-circle by the CO_2 and H_2O flow rate increase. This reflects kinetic aspects of the anode reaction wherein CO_2 and H_2O additions reduce the mass-transfer resistance at the anode and the lower frequency semi-circle represents the gas phase mass-transfer effect.

In this work, results from SSP, RA, ISA, and EIS consistently shown that the CO_2 and H_2O species in the anode are related to the anodic reaction and increase of their flow rates reduces mass-transfer resistance and, subsequently, overpotential.

Conclusion

Anodic reaction characteristics have been investigated through the overpotential at standard (H_2:CO_2:H_2O = 0.69:0.17:0.14 atm) and equal (H_2:CO_2:H_2O = 0.33:0.33:0.33 atm) compositions while maintaining a constant H_2 flow rate. Steady state polarization, reactant gas addition (RA), inert gas step addition (ISA), and electrochemical impedance spectroscopy (EIS) have been employed in this work. These methods revealed that the anodic overpotential is comprised of each overpotential due to the reactant species, H_2, CO_2, and H_2O. Anodic overpotential decreases with increasing flow rate of CO_2 and H_2O species, indicating that the relatively large overpotential at the standard composition is attributed to the low flow rate of those species. Overpotential due to the H_2 species increases at a larger amount of CO_2 and H_2O, likely due to reduced H_2 diffusivity by the enlarged CO_2 and H_2O amounts. ISA gave quantitative information of overpotential at both gas compositions. EIS also showed the flow rate effect of CO_2 and H_2O clearly on the Cole-Cole plot. The lower frequency half circle is reduced by the increase of CO_2 and H_2O flow rates without affecting the high frequency semi-circle.

References

1. J. R. Selman and H. C. Maru, in Advances in Molten Salt Chemistry, Vol. 4, G. Mamantov and J. Braunstein, Ed., p.159, Plenum Press, New York (1981).
2. J. R. Selman, in Fuel Cell Systems, Eds. L. J. M. J. Blomen and M. N. Mugerwa, Plenum Press, NY (1993).
3. F. Yoshiba, Y. Mugikura, Y. Izaki, and T. Watanabe, in Proceedings of 10th Fuel Cell Symposium, B9, FCDIC, Tokyo (2003).
4. P. G. P. Ang and A. F. Sammells, *J. Electrochem. Soc*., **127**, 1289 (1980).
5. C. Y. Yuh and J. R. Selman, *J. Electrochem. Soc*., **138**, 3642 (1991).
6. H. Morita, Y. Mugikura, Y. Izaki, T. Watanabe, and T. Abe, Denki Kagaku, **65**, 740 (1997).
7. G. Lindbergh, M. Olivry, and M. Sparr, *J. Electrochem. Soc.*, **148**, A411 (2001).
8. C.-G. Lee, B.-S. Kang, H.-K. Seo and H.-C. Lim, *J. Electroanal. Chem*., **540**, 169 (2003).
9. C.-G. Lee, H.-C. Lim, and J.-M. Oh, *J. Electroanal. Chem*., **560**, 1 (2003).
10. C.-G. Lee, H.-K. Ahn, K.-S. Ahn, and H.-C. Lim, *J. Electroanal. Chem*., **568**, 13 (2004).
11. C.-G. Lee and H.-C. Lim, *J. Electrochem. Soc.*, **152**, A219 (2005).
12. C.-G. Lee, H. Nakano, T. Nishina, I. Uchida, Y. Izaki, and S. Kuroe, Denki Kagaku, **64**, 486 (1996).
13. H. Morita, H. Nakano, Y. Mugikura, Y. Izaki, T. Watanabe, and I. Uchida, *J. Electrochem. Soc*., **150**, A1693 (2003).
14. E. L. Cussler, Diffusion, mass transfer in fluid systems, 2nd Ed., Cambridge University Press (1997).